

Radio and Submillimeter Continuum Observations of High-Redshift Galaxies

Wei-Hao Wang¹, Amy J. Barger^{2,3,4}, Lennox L. Cowie⁴,
Chian-Chou Chen⁴, Jonathan P. Williams⁴, and Frazer N. Owen⁵

¹Institute of Astronomy and Astrophysics, Academia Sinica,
P.O. Box 23-141, Taipei 10617, Taiwan
email: whwang@asiaa.sinica.edu.tw

²Department of Astronomy, University of Wisconsin-Madison,
475 N. Charter Street, Madison, WI 53706, USA

³Department of Physics and Astronomy, University of Hawaii,
2505 Correa Road, Honolulu, HI 96822, USA

⁴Institute for Astronomy, University of Hawaii,
2680 Woodlawn Drive, Honolulu, HI 96822, USA

⁵National Radio Astronomical Observatory,
P.O. Box 0, Socorro, NM 87801, USA

Abstract. Observing galaxies in the radio and submillimeter continuum has the advantage of being unaffected by dust extinction, which is a major drawback of studying galaxy evolution using optical data. Submillimeter single-dish surveys have made tremendous progress in understanding the high-redshift dusty population, but the low angular resolution of single-dish telescopes has also hampered these studies. Our recent JCMT and SMA imaging of high-redshift submillimeter sources revealed $z > 4$ objects that are radio and optically faint. Such objects cannot be easily identified with the combination of submillimeter single-dish and radio imaging. We also found a large fraction of multiple objects that are blended in single-dish images. Such objects may be early-stage mergers, or dusty starbursts in group environments. Since our work, larger surveys with PdBI and ALMA have been carried out to further address these issues. Additional to submillimeter imaging, future ultradeep EVLA imaging at 20 cm can also detect large samples of ultraluminous star forming galaxies at $z \gtrsim 2$. Sensitivities in radio and submillimeter observations have different redshift and dust temperature dependencies. Radio observations are also less affected by confusion. It will be necessary to combine deep surveys in both wavebands in order to achieve a more complete picture of the evolution of high-redshift star forming galaxies.

Keywords. galaxies: high-redshift — submillimeter — radio continuum: galaxies

1. Introduction

The far-infrared (FIR) portion of the extragalactic background light (EBL) has an observed strength comparable to that in the optical and near-infrared (NIR; e.g., Dole *et al.* 2006). This implies a large fraction of cosmic star formation being hidden by dust, and that a complete picture of galaxy evolution requires an understanding of infrared luminous galaxies. To understand the evolution of the galaxies that give rise to the FIR EBL, the next crucial step is to resolve the background into discrete sources and to identify dusty galaxies in multiwavelength galaxy evolution surveys.

From the ground, the FIR EBL can be studied through the submillimeter and millimeter (submm/mm) windows. In this waveband, we do not observe the peak of the

EBL, which is at around $200\ \mu\text{m}$. However, the strong negative K -correction in the Rayleigh-Jeans portion of the dust spectral energy distribution (SED) makes the observed submm/mm flux almost invariant from $z \sim 1$ to $z > 5$ (Blain & Longair 1993). This is not the case for wavebands of $\lesssim 300\ \mu\text{m}$. For example, *Herschel* SPIRE surveys have a strong tendency of picking up objects at $z < 1.5$ (e.g., Casey *et al.* 2012). Another factor that favors submm/mm observations is confusion. Recent deep *Herschel* SPIRE observations were only able to resolve small fractions (15%, 10%, and 6%) of the FIR EBL at 250, 350, and 500 μm (Oliver *et al.* 2010), due to the confusion limit. On the other hand, ground-based submm/mm single-dish telescopes have angular resolutions several times higher than that of *Herschel*, and are less affected by confusion. Roughly 20%–30% of the 850 μm and 1100 μm EBL can be directly resolved by various instruments (SCUBA, AzTEC, MAMBO, and LABOCA; see, e.g., Coppin *et al.* 2006; Hatsukade *et al.* 2011). Recent SCUBA-2 observations at 450 μm start to resolve even larger fractions of the EBL (e.g., Chen *et al.* 2011), because of its higher angular resolution. Because of the sensitivity to high-redshift galaxies and the higher resolution achievable from the ground, resolving the submm/mm portion of the FIR EBL is of great interest.

Another important waveband for probing high-redshift dusty galaxies is radio continuum. The steep spectral slope of radio synchrotron emission produces a positive K -correction and makes radio observations less sensitive to high-redshift galaxies. However, radio interferometric imaging has the advantage of high angular resolution ($\sim 1''\text{--}2''$), which reduces the effect of confusion and the problems of counterpart identification at other wavebands. Furthermore, there is a tight correlation between radio power and FIR luminosity of local star forming galaxies (see a review in Condon 1992), which is insensitive to dust temperature. The radio–FIR correlation also does not appear to evolve strongly at high redshift (e.g., Ivison *et al.* 2010; Bourne *et al.* 2011). Therefore, radio continuum observations can effectively pick up FIR luminous objects, and are highly complementary to submm/mm surveys.

In this paper, we summarize our studies of high-redshift dusty objects using various ground-based submm/mm and radio instruments, and discuss several outstanding issues. In Section 2, we describe our submillimeter surveys with JCMT SCUBA and SCUBA-2 and with the Submillimeter Array (SMA). In Section 3, we discuss the prospect of extremely deep radio continuum imaging. We conclude in Section 4.

2. Submillimeter Surveys

Our group has carried out various SCUBA 850 μm surveys in blank fields (e.g., Barger *et al.* 1998; Wang, Cowie, & Barger 2004) and lensing cluster fields (Cowie, Barger, & Kneib 2002). We also followed up the SCUBA samples in the Great Observatories Origins Deep Survey–North (GOODS-N, see below) and in lensing cluster fields (Chen *et al.* 2011) using the SMA with $\sim 1''\text{--}2''$ resolution at $\sim 345\ \text{GHz}$. The high resolution of the SMA allows us to unambiguously determine the counterparts to the SCUBA sources and to avoid any bias introduced by identifying counterparts at a different wavebands (e.g., the radio bias against high-redshift sources, caused by the positive K -correction). The improved astrometry also allows us to better constrain the lensing factors for sources lensed by clusters.

Barger *et al.* (2012) summarize the results of our SMA followup of the GOODS-N SCUBA sample of Wang *et al.* (2004). Out of the $16 > 4\sigma$ sources with 850 μm fluxes greater than 3 mJy in Wang *et al.* (2004), 12 were detected by the SMA. Many of the SMA detected sources have unexpected properties that cannot be revealed with conventional radio identification:

High-Redshift Objects — The submillimeter waveband has a unique advantage of a large K -correction that nearly cancels the effect of luminosity distance. Therefore, bright submillimeter objects that are faint in all other wavelengths are candidates of high-redshift objects. In our SMA survey, we found SMGs that are extremely optically faint and radio faint, and cannot be easily identified in any other wavebands (GOODS 850-5, Wang *et al.* 2007; HDF850.1, Cowie *et al.* 2009; also see Younger *et al.* 2007; 2009). GOODS 850-5 was later confirmed to be at $z = 4.04$ (Daddi *et al.* 2009) and HDF850.1 was confirmed to be at $z = 5.18$ (Walter *et al.* 2012), both by CO line searches with PdBI. These results show that radio identification are biased against high-redshift objects, and also show the importance of the ability to blindly detect molecular lines from high-redshift objects.

Multiplicity — Two of our SCUBA sources, GOODS 850-11 and 850-13 (Figure 1) were resolved by the SMA into five widely separated ($\sim 20''$) faint objects (Wang *et al.* 2011). The two SCUBA sources have blended 850 μm fluxes of 10.8 and 7.0 mJy, and the five SMA sources have fluxes of 3–6 mJy. This suggests that either the number of fainter objects (a few mJy) was under-estimated in previous counts, or that there is clustering in group scale. Furthermore, four additional SCUBA sources in our sample, GOODS 850-7, 850-9, 850-15, and 850-17, have radio counterparts that appear to be close radio pairs with red NIR colors (Figure 1). For each of GOODS 850-7, 850-9, and 850-17, our SMA imaging detected one galaxy in the radio pair. For GOODS 850-15, our SMA imaging detected both radio sources. These are likely early-stage mergers, or SMGs lensed by foreground galaxies. Hayward *et al.* 2011 argued that SMGs can be either tidally driven starbursts in mergers, or blended disks in early-stage interacting pairs. The large fraction of multiple radio and submillimeter sources in our SMA sample (six out of twelve) appears to support the Hayward *et al.* scenario.

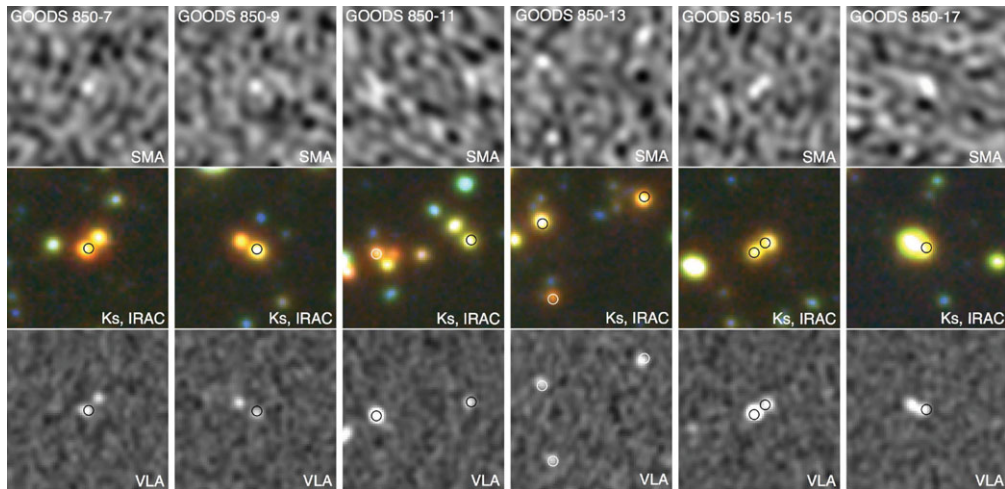


Figure 1. Multiple galaxies in our SMA sample. The full sample of our GOODS-N SMA is described in Barger *et al.* (2012). Here is a subsample of multiple SMA detections or radio pairs. All the panels have 25 arcsec on a side. The top panels are our SMA images at 345 GHz. The middle panels are 2.1–8.0 μm near-infrared pictures. [See the electronic edition for the color version of the pictures, which are made with K_s (blue), *Spitzer* IRAC 3.6+4.5 μm (green), and IRAC 5.8+8.0 μm (red) images.] The bottom panels are the latest ultradeep VLA 20 cm images (F. Owen *et al.* 2012, in prep.).

Our SMA imaging of both high-redshift SMGs and multiple objects show the limit of single-dish studies and radio identifications. It is thus important to directly identify

submillimeter single-dish sources with submillimeter interferometry. Recent results from PdBI (Smolčić *et al.* 2012) and ALMA (Karim *et al.* 2012) with larger samples both found multiple objects. The ALMA imaging of Karim *et al.*, however, are not consistent with our SMA results. Among their 69 ALMA detected LABOCA sources, the authors do not find any single sources brighter than 9 mJy. All bright LABOCA sources are resolved by ALMA into multiple ones. In contrast, we detected three single > 9 mJy sources among our 12 SMA detected SCUBA sources (see also, Younger *et al.* 2007, 2009). It is unclear whether cosmic variance alone can explain this discrepancy. Another subtle issue is the difference in beam sizes. The primary beam of ALMA is only 50% of that of SMA. Widely separated objects (such as GOODS 850-11 and 850-13 in Figure 1) may not be easily detected by ALMA. To properly address these issues, we clearly need larger submm/mm samples, which are being produced by new-generation single-dish surveys (e.g., the SCUBA-2 survey of Chen *et al.* 2012). Blind ALMA deep surveys may also be necessary to address the issues of widely separated objects.

Finally, new-generation single-dish instruments, such as SCUBA-2 and AzTEC on the LMT, will provide insight into the typical galaxies that give rise to the submm/mm EBL. At 850 μm , blank-field SCUBA/SCUBA-2 surveys are only able to detect objects of $\gtrsim 2$ mJy. These objects only comprise $\sim 20\%-30\%$ of the EBL at this waveband (Coppin *et al.* 2006). The confusion is less an issue at 450 μm , due to the higher resolution. In our latest SCUBA-2 lensing cluster survey (Chen *et al.* 2012), we had resolved $\sim 47\%-61\%$ of the 450 μm EBL. Based on this work, we further estimate that a reasonably deep (> 10 hours of integration) 450 μm SCUBA-2 *blank-field* image can resolve $\sim 50\%$ of the EBL. This is higher than the resolved fraction at 850 μm , and is much higher than the fraction of 500 μm EBL resolved by *Herschel* (6%, Oliver *et al.* 2010). We therefore expect SCUBA-2 to make major impact at 450 μm . On the other hand, a confusion limited SCUBA-2 450 μm image (with a detection limit of ~ 2 mJy) can fully resolve the EBL, but will require several hundreds of hours of integration. This will be a very challenging project on SCUBA-2 due to the huge observing time.

3. Deep Radio Imaging

Deep imaging in the radio wavelengths (e.g., 20 cm) is highly complementary to FIR and submm/mm imaging. First, radio images can have arcsec and sub-arcsec resolutions. They are less affected by confusion, and can detect galaxy populations with much higher surface densities on the sky. Second, submm/mm observations are biased toward objects with cooler dust (e.g., Magnelli *et al.* 2012; also see Chapman *et al.* 2004). This bias is not obvious in the radio, given that the local radio–FIR correlation is insensitive to dust temperature. The main disadvantage of radio observations is its low sensitivity to high-redshift objects (Figure 2) due to the synchrotron spectral slope.

The deepest VLA image (Owen & Morrison 2008) and recent EVLA images (e.g., Figure 1) at 20 cm have reached detection limits of $\gtrsim 10 \mu\text{Jy}$ (Figure 2). This allows to detect $L_{\text{IR}} = 10^{12} L_{\odot}$ objects at $z \gtrsim 2$, which include the majority of disk-mode star forming galaxies and merger driven starbursts at the peak of the cosmic star formation (e.g., Rodighiero *et al.* 2011). The source density at this flux limit is approximately 10^4 deg^{-2} , already higher than the confusion limits of FIR and submm/mm single-dish surveys. Future EVLA surveys can push the detection limits to a few to ~ 10 times deeper, before reaching the natural confusion limit.

The high angular resolution in the radio also helps stacking analyses. When angular resolution is poor, there is always the worry about source clustering at scales comparable to the beam sizes of the observations, which may lead to overestimated stacking

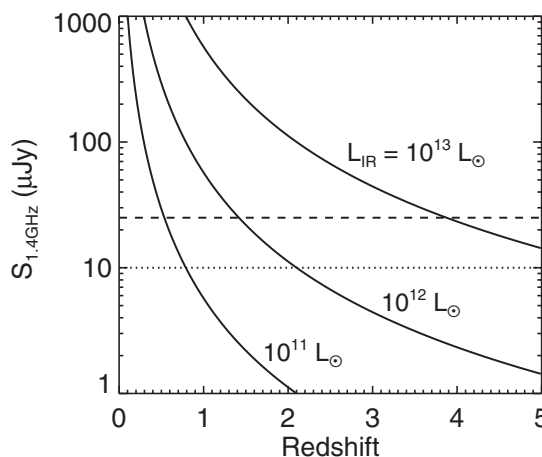


Figure 2. Observed 20 cm flux vs. redshift. The curves are 20 cm fluxes for galaxies with $L_{\text{IR}} = 10^{11}, 10^{12}$, and $10^{13} L_{\odot}$, derived based on the local radio–FIR correlation in Wang, Barger, & Cowie (2012). The dashed line shows the typical detection limit of a deep VLA image (e.g., Morrison *et al.* 2010). The dotted line shows the detection limit of the deepest VLA image (Owen & Morrison 2008) and the limit that has been achieved by the EVLA in the mean time (e.g., the GOODS-N image in Figure 1).

fluxes. Our recent detections of multiple SMGs and radio pairs (Section 2) further deepen this worry. With the arcsec resolution in the radio, we are probing the scale of galaxy disks at high redshift. This makes the interpretation of the stacking results much more straightforward. Our 20 cm stacking analyses successfully detected ~ 200 extremely red objects selected in the NIR K_S and $4.5 \mu\text{m}$ bands, and showed that such objects contribute significantly to the cosmic star formation history (Wang, Barger, & Cowie 2012). The deep 20 cm stacking analyses of Ho *et al.* (2010) on a sample of ~ 3500 *HST* ACS selected $z \sim 4$ Lyman-break galaxies in the GOODS-N/S reached a stacked 20 cm rms sensitivity of $0.15 \mu\text{Jy}$, corresponding to star formation rates (SFRs) of $\sim 10 M_{\odot} \text{ yr}^{-1}$ (see also, Carilli *et al.* 2008). This is very close to the SFR limits in sensitive rest-frame UV observations of high-redshift galaxies, meaning that we can start to verify the SFR measured in the optical using radio observations.

4. Final Remarks

Thanks to single-dish telescopes including *Herschel*, the progress in understanding high-redshift dusty star forming galaxies is remarkable in the last decade. However, the studies overwhelming focus on bright objects, which is a fundamental limit of single dishes. There is still a lack of knowledge on the typical galaxies that give rise to the bulk of the FIR EBL. EVLA surveys and ultimately ALMA surveys at various submm/mm bands are needed to address this. Both instruments will be in full operation very soon, and we expect to see dramatic progress in the coming years.

References

- Barger, A. J., Cowie, L. L., Sanders, D. B., Fulton, E., Taniguchi, Y., Sato, Y., Kawara, K., & Okuda, H. 1998, *Nature*, 394, 248
 Barger, A. J., Wang, W.-H., Cowie, L. L., Owen, F. N., Chen, C.-C., & Williams, J. P. 2012, *ApJ*, in press (arXiv:1209.1626)

- Blain, A. W. & Longair, M. S. 1993, *MNRAS*, 264, 509
Bourne, N., *et al.* 2011, *MNRAS*, 410, 1155
Casey, C. M., *et al.* 2012, *ApJ*, *in press* (arXiv:1210.4928)
Carilli, C. L., *et al.* 2008, *ApJ*, 689, 883
Chapman, S. C., Smail, I., Blain, A. W., & Ivison, R. J. 2004, *ApJ*, 614, 671
Chen, C.-C., Cowie, L. L., Wang, W.-H., Barger, A. J., & Williams, J. P. 2011, *ApJ*, 733, 64
Chen, C.-C., Cowie, L. L., Barger, A. J., Casey, C. M., Lee, N., Sanders, D. B., Wang, W.-H., & Williams, J. P. 2012, *ApJ*, submitted (arXiv:1209.4377)
Condon, J. J. 1992, *ARA&A*, 30, 575
Coppin, K., *et al.* 2006, *MNRAS*, 372, 1621
Cowie, L. L., Barger, A. J., & Kneib, J.-P. 2002, *AJ*, 123, 2197
Cowie, L. L., Barger, A. J., Wang, W.-H., & Williams, J. P. 2009, *ApJ*, 697, L122
Daddi, E., Dannerbauer, H., Krips, M., Walter, F., Dickinson, M., Elbaz, D., & Morrison, G. E. 2009, *ApJ*, 695, L176
Dole, H., *et al.* 2006, *A&A*, 451, 417
Hatsukade, B., *et al.* 2010, *ApJ*, 711, 974
Hayward, C. C., Kereš, D., Jonsson, P., Narayanan, D., Cox, T. J., & Herquist, L. 2011, *ApJ*, 743, 159
Ho, I.-T., Wang, W.-H., Morrison, G. E., & Miller, N. A. 2010, *ApJ*, 722, 1051
Ivison, R. J., *et al.* 2010, *MNRAS*, 402, 245
Karim, A., *et al.* 2012, *MNRAS*, submitted (arXiv:1210.0249)
Magnelli, B., *et al.* 2012, *A&A*, 539, 155
Morrison, G. E., Owen, F. N., Dickinson, M., Ivison, R. J., & Ibar, E. 2010, *ApJS*, 188, 178
Oliver, S. J., *et al.* 2010, *A&A*, 518, L21
Owen, F. N. & Morrison, G. E. 2008, *AJ*, 136, 1889
Rodighiero, G., *et al.* 2011, *ApJ*, 739, L40
Smolčić, V., *et al.* 2012, *A&A*, *in press* (arXiv:1205.6470)
Walter, F., *et al.* 2012, *Nature*, 486, 233
Wang, W.-H., Cowie, L. L., & Barger, A. J. 2004, *ApJ*, 613, 655
Wang, W.-H., Cowie, L. L., van Saders, J., Barger, A. J., & Williams, J. P. 2007, *ApJ*, 670, L89
Wang, W.-H., Cowie, L. L., Barger, A. J., & Williams, J. P. 2011, *ApJ*, 726, L18
Wang, W.-H., Barger, A. J., & Cowie, L. L. 2012, *ApJ*, 744, 155
Younger, J. D., *et al.* 2007, *ApJ*, 671, 1531
Younger, J. D., *et al.* 2009, *ApJ*, 704, 803